www.vbripress.com/aml, DOI: 10.5185/amlett.2016.6497 Published online by the VBRI Press in 2016

Neodymium doped ZrO_2-graphene oxide nanocomposites: A promising photocatalyst for photodegradation of Eosin Y dye

M. Mzoughi[1, 2], William. W. Anku[1], Samuel O. B. Oppong[1], Sudheesh K. Shukla[1, 3*], Eric S. Agorku[1], Penny P. Govender[1*]

[1]*Department of Applied Chemistry, University of Johannesburg, P.O. Box 17011, Doornfontein 2028, Johannesburg, South Africa*
[2]*Ecole Nationale Superieure des Ingénieurs en Arts Chimiques et Technologiques, INP-Toulouse, 4, allée Émile-Monso, BP 44362, 31030, Toulouse, France*
[3]*Vinoba Bhave Research Institute, Sirsa Road, Saidabad, Allahabad 221508, India*

[*]Corresponding author. Tel: (+27) 115599013; E-mail: sudheeshkshukla@gmail.com; pennyg@uj.ac.za

Received: 01 March 2016, Revised: 11 June 2016 and Accepted: 22 June 2016

ABSTRACT

Purification of industrial wastewater from dyes receiving increasing attentions. The aim of the present manuscript was to fabricate graphene based nanocomposites using a homogeneous and facile approach. Co-precipitation method was used to synthesize zirconium oxide (ZrO_2) and neodymium doped ZrO_2-graphene oxide (Nd-ZrO_2-GO) nanocomposites with varying weight percent concentrations of neodymium to investigate the increasing photocatalytic activity. The Nd-ZrO_2-GO catalysts were characterized using X-ray powder diffraction (XRD), Fourier transform infrared (FTIR) spectroscopy, scanning electron microscopy (SEM), transmission electron microscopy (SEM), and ultra violet-visible (UV-vis)-spectroscopy to evaluate their optical, morphological and structural properties respectively. The photocatalytic degradation potential of the nanocatalyst was assessed by the degradation of Eosin Y dye in aqueous solution under simulated solar light irradiation. The Nd-ZrO_2-GO was observed to have higher photocatalytic degradation potential than the bare ZrO_2. The most efficient photocatalyst for the degradation of Eosin Y dye was 0.3 % Nd-ZrO_2-GO with about 80 % efficiency within 180 min and a Ka value of 4.19 x10^{-3}. Nd-ZrO_2-GO catalyst would be considered as efficient photocatalyst to degrade the industrial dyes (Eosin Y) avoiding the dreary filtration steps. Copyright © 2016 VBRI Press.

Keywords: Photocatalysis; polymer-metal nanocomposites; graphene oxide; eosin Y; dye degradation; photodegradation.

Introduction

It has been shown in recent times that photocatalytic degradation with metal oxide semiconductors such as ZrO_2 can be used effectively to remove a wide variety of organic pollutants from water **[1, 2]**. This process generates strong oxidizing and reducing species which attach and convert the organic pollutants into simple and harmless products such as carbon dioxide and water. Semiconductor photocatalysis is therefore regarded as being the most efficient waste water treatment technology, and environmentally friendly **[3]**.

Semiconductors such as TiO_2, ZnO, ZnS, and ZrO_2 have been tested as photocatalysts as a result of their electronic structure which is influenced by filled valence band and an empty conduction band **[4]**. ZrO_2 has been extensively studied as a photocatalyst because of its efficient ionic conductivity due to oxygen vacancies. Another property is its high activity in photocatalysis, which is a good starting point to get an optimized product **[5]**. However, the biggest disadvantage is its photosensitivity to solar light. Zirconium's wide band gap (5-5.85 eV) limits its activity to UV light which represents only 4 % of solar light **[6]** affecting its efficiency as a photocatalyst. Recombination of the electron-hole pairs after generation is another problem hindering the efficiency of ZrO_2 as a photocatalyst. It is therefore necessary to modify ZrO_2 in such a way as to reduce its wide band gap and minimize the recombination rate of the photogenerated electrons and holes. Recently, graphene attracted scientific interest due to tits excellent specific surface charge, promising thermal as well electrical conduction and carrier's motilities. Due to the hexagonal honeycomb like network, the sp2-bonded carbon lattice has exceptional electrical and spacious delocalized π-bond which enhances its conductivity capacity and structural stability. The O_2-containing functional groups on the surface of graphene oxide, recommended its candidature for a good supporting materials for other entities of nanomaterials. In this respect, anchoring well-organized Nd-ZrO_2- nanostructures over the GO sheet can be efficiently utilize to attain for a promising photocatalytic concert **[7-9]**. The wide band gap of ZrO_2 can be reduced by modifying it with graphene oxide **[10]**. With a relatively small band gap coupled with high optical and mechanical properties, graphene oxide based photocatalyst are expected to be visible light active and exhibit synergistic properties of the individual materials.

The reactivity of the photocatalyst can be improved if the electron could be spontaneously trapped by an electrical insulator or by a default **[11]**. This default can be an anion vacancy which is created by the replacement of a host cation by a dopant. An electron trapped by this anionic vacancy is very movable which create a high activity within the reaction medium **[12]**.

Modification of ZrO_2 with graphene oxide and a metal ion is therefore expected to result in an ideal ZrO_2 photocatalyst for the effective removal of organic pollutants from water. This study therefore involved the synthesis of Nd doped ZrO_2-GO nanocomposites with varying percentage concentrations of Nd through the homogeneous co-precipitation method. The photocatalytic degradation potential of the nanocomposites against Eosin dye as a model organic pollutant is also discussed.

Experimental

All chemicals were obtained from Sigma-Aldrich and used without further purification.

Synthesis of graphene oxide

Graphene oxide synthesis was carried out based on modified Hammers methods **[13]**. Typically, a H_2SO_4/H_3PO_4 mixture in the ratio of 9:1 (360:40 mL) was added to a mixture consisting of 3.0 g graphite flakes and 18. 0 g $KMnO_4$ and the mixture heated at 500 ^oC with continuous magnetic stirring for 12 h. After cooling the reaction system to room temperature, 3 mL of 30 % H_2O_2 and 400 mL deionized water was added slowly followed by centrifugation at 7, 500 rpm for 15 min at 4^oC. The supernatant was then decanted and the solid material washed several times with 1000 mL deionized water and 30 % HCl. The solid material was again mixed with 1000 mL deionized water and centrifuged. The residual solid material was finally coagulated with 200 mL petroleum ether and filtered through a Teflon membrane filter (1 µm pore size). The obtained graphene oxide was then vacuum-dried overnight at room temperature.

Synthesis of Nd–ZrO_2–GO nanocomposite

This synthesis followed the method of Agorku *et al.* 2015 **[14]**. This process involved the dispersion and sonication of 9.81 g of Zr $(NO_3)_2.6H_2O$ and calculated amounts of Nd $(NO_3)_3.6H_2O$ in 50 mL deionized water in order to obtain 0.3 %, 0.6 & and 1.0 % Nd doped ZrO_2 nanoparticle. The mixture was later stirred magnetically for 1 h after which 0.116 mL of GO representing 0.5 % was added and the mixture stirred at 50 °C for 2 h.

The Nd–ZrO_2–GO nanoparticle was precipitated through drop wise addition of 3M KOH with continuous magnetic stirring until pH between 9 and 10 was obtained. The Nd–ZrO_2–GO composite was then separated by centrifugation and washed several times with a mixture of deionized water and ethanol to remove nitrate and chloride ions. The synthesized Nd-ZrO_2-GO nanoparticle was dried overnight at 90 °C and calcined at 300°C for 3 h. ZrO_2 and ZrO_2–GO were also synthesized in a similar manner without the addition of either $Nd(NO_3)_3.6H_2O$ or both GO and $Nd(NO_3)_3.6H_2O$.

Evaluation of photocatalytic activity

The photocatalytic activity of each photocatalyst was estimated through degradation of Eosin Y aqueous solution (100mL; 20ppm) with 100 mg of each catalyst under simulated solar light with continuous magnetic stirring at room temperature. The catalyst-dye mixture was first kept in the dark at room temperature for 30 min before illumination with light filtered with a dichroic UV filter with wavelength of 420 nm. The light was produced using a Port 9600 Full Spectrum Solar Simulator equipped with 150 W ozone free xenon lamp that was set at a distance of 10 cm to produce only 1 sun intense beam to study photodegradation of dyes. Exactly 5 mL aliquots of the suspensions were taken from the reaction medium every 30 min for 3h with a syringe fitted with a 0.4 µm PVDF membrane filter. Concentration of Eosin Y in every aliquot was determinate with a Shimadzu UV-2450 spectrophotometer at λ = 516 nm. The kinetic study and degradation performance was determinate in term of decolorization efficiency.

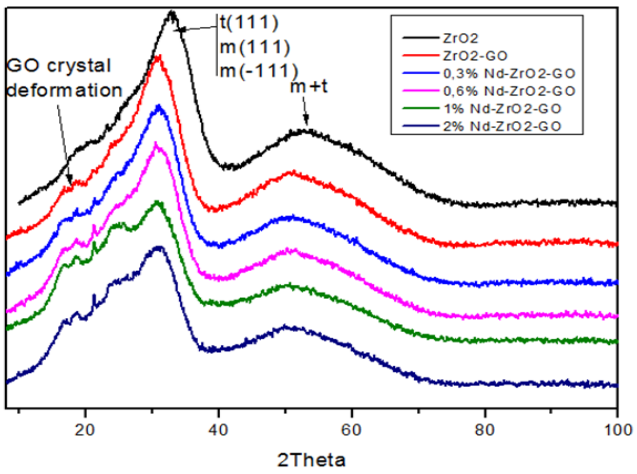

Fig. 1. XRD pattern of Nd doped-ZrO_2-GO.

Characterization

Fourier transform infrared spectroscopy (FTIR) spectra of the samples were recorded on a PerkinElmer FTIR spectrometer (Spectrum 100). X-ray diffraction (XRD) measurements were accomplished on Rigagu Ultima IV X-ray diffractometer at 40 kV and 30 mA with Cu Ka radiation (k = 0.15406) with K-beta filter. Measurements were performed using a scintillation counter in the range of 5–100 at a speed of 2.0 deg/min. Scanning electron microscopy (SEM) studies were acquired on a TESCAN (Vega 3 XMU). The elemental composition of the samples was determined using energy dispersed X-ray spectroscopy (EDX) attached to SEM. Optical properties were investigated using UV–vis absorption and UV–vis diffuse reflectance spectroscopy on a Shimadzu UV-2540 (Japan) with $BaSO_4$ as the reflectance standard.

Results and discussion

XRD analysis

Fig. 1 shows the XRD patterns of ZrO_2, ZrO_2-GO and Nd-doped ZrO_2-GO nanoparticles. Two broad peaks, at around

30.1° and 50.2° are observable. These peaks reveal that the crystalline structure of the nanocomposites is in the amorphous state because of the broadness of the peaks. No intense diffraction peak could validate the presence of GO which may be possibly due to its low concentration (0.5 %) and therefore its relatively low diffraction intensity in the nanocomposites **[15]**.

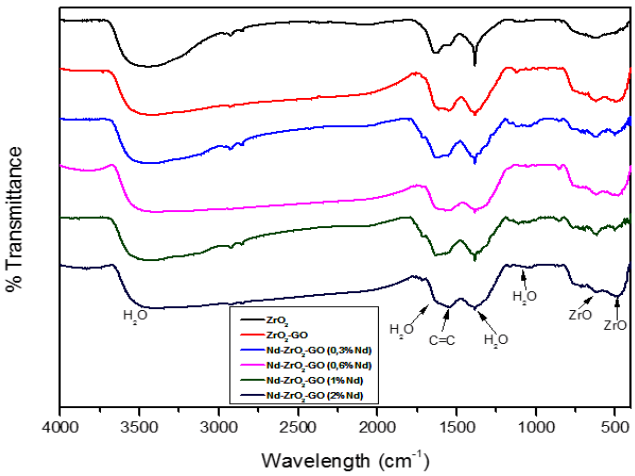

Fig. 2. FTIR of Nd doped ZrO_2-GO.

FTIR

The FTIR spectrum provides information on chemistry of nanoparticles shows the FTIR spectra of the ZrO_2, ZrO_2-GO and Nd-doped ZrO_2-GO nanoparticles (**Fig. 2**). Peaks due to bending vibration of O-H are observed between 3450 cm^{-1} and 3350 cm^{-1}, and 1635 cm^{-1} and 1620 cm^{-1}. These OH groups are ascribed to water molecule adsorbed from the environment. GO is characterized by peaks between 1635 and 1620 cm^{-1}, mainly attributed to in plane C=C band vibrations of aromatic groups **[16]**. Notably, all the above peaks are observed for the ZrO_2–GO and Nd-doped ZrO_2–GO as well except that these observed peaks were slightly shifted to lower wavelengths. This shift could be due to the interaction of ZrO_2 with GO in the composites. The absorptions at 485 and 627 cm^{-1} are attributed to stretching vibrations of ZrO_2 bonds **[10]**, which shifted to lower wave numbers in the modified nanocomposites indicating the interaction between GO, Nd and ZrO_2.

TEM and SEM studies

TEM and SEM were performed to assess the size, uniformity, morphology and microstructure of the nanoparticles. The TEM, SEM and EDX images of ZrO_2 and Nd doped ZrO_2-GO nanoparticles are shown in **Fig. 3**. The SEM image of ZrO_2 (**Fig. 3a)** clearly shows the formation of small size $ZrO_2$with distinct grains. **Fig. 3b** shows that the Nd-ZrO_2nanoparticles are enclosed in GO. All the nanocomposites exhibited regular morphology irrespective of Nd doping. The EDX spectrum estimated the amount of each element in the Nd doped ZrO_2-GO photocatalysts. This spectrum confirms the presence of Nd, C, Zr and O in the catalysts. It also indicates that the main contents are Zr and O whereas Nd is in low concentration but close to what was expected.

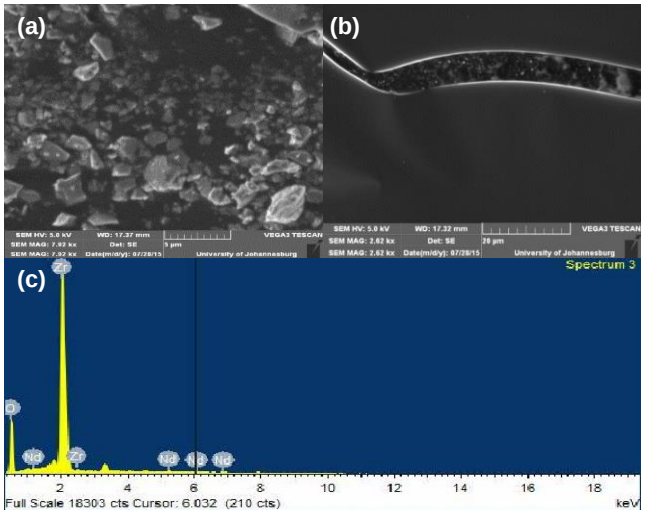

Fig. 3. SEM image of (a) ZrO_2, (b) Nd doped ZrO_2-GO and (c) EDX spectrum of Nd doped ZrO_2-GO.

Optical studies

The UV-visible absorption spectra of the samples revealed that modification of ZrO_2using Nd and GO resulted in enhanced visible light absorption of ZrO_2. **Fig. 4** shows the absorption spectrum of the synthesized ZrO_2, ZrO_2-GO and Nd doped ZrO_2-GO nanoparticles. The spectra shows a significant increase in absorption of light in the entire visible light region by the doped catalysts over pure ZrO_2.This phenomenon is due to the multiplication of discrete energy levels **[5]**, which decrease original zirconia band gap. It is also attributed to Nd doping and its ability to act as electron scavenger to reduce electron-hole recombination rate.

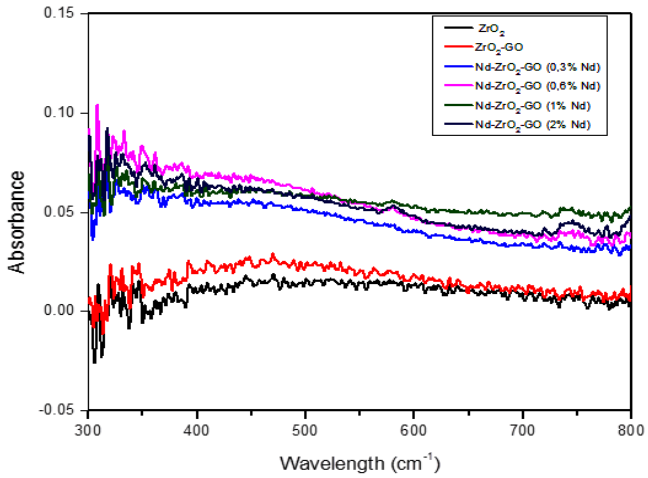

Fig. 4. UV-visible absorbance spectra of Nd doped ZrO_2-GO.

Even though introduction of Nd and GO resulted in improved visible light absorption, there appears to be no direct link between quantity of Nd doped and absorbance results i.e, an increase in Nd concentration did not necessarily result in increased visible light absorption of the catalysts.

With regards to reflectance, the pure zirconia is the most reflected of the catalysts in the entire visible light region (**Fig. 5)**. The modified catalysts were less reflected in

comparison to pure ZrO_2. However, the peak positions further shifted a bit to a shorter wavelength due to the addition of GO and Nd.

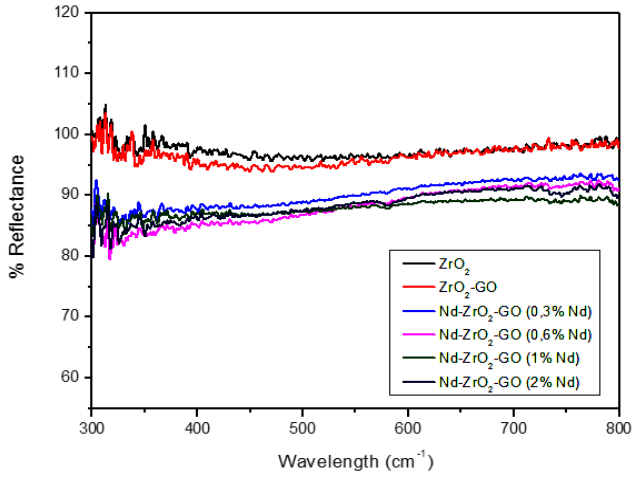

Fig. 5. UV Reflectance spectra of Nd doped ZrO_2-GO.

Photocatalytic activity

The photocatalytic activity of the prepared Nd-ZrO_2–GO nanocomposites was determined using the degradation of 20 ppm aqueous solutions of Eosin Y dye as a model for organic pollutants. The degradation was carried out under simulated solar light. The significant optical absorption peak of Eosin Y at 516 nm was used to monitor the photodegradation process. The ZrO_2-GO and the Nd-ZrO_2-GO showed improved performance over the bare ZrO_2. The peak evolution of Eosin Y solution degraded by the 0.3 %Nd-ZrO_2-GO is given in **Fig. 6**. The efficiency of the photocatalyst is indicated by the absorbance peak evolution from 0 min to 180 min. The gradual decrease in absorbance of the optical absorption peak with time indicates the gradual degradation of the dye with increasing time.

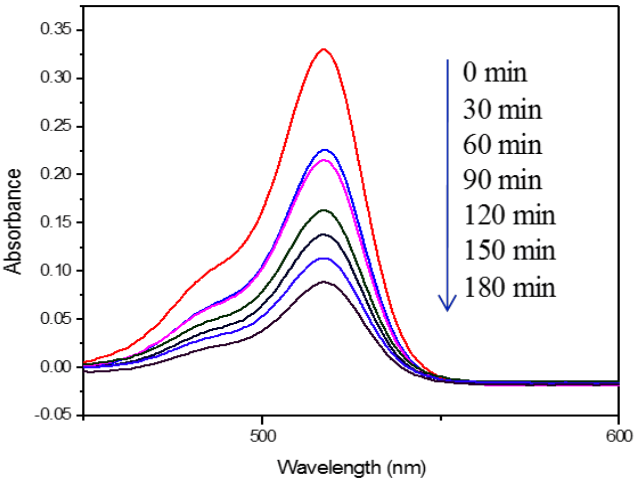

Fig. 6. Eosin Y photodegradation profile using 0.3% Nd doped ZrO_2-GO.

Fig. 7 represents the kinetics of Eosin Y degradation. **Fig. 7** clearly shows that 0.3% Nd- ZrO_2-GO showed the best photocatalytic activity under solar light beam. This observation is not explained in terms of its absorbance properties, but the ratio of Zr and Nd could be the cause of this performance. It can therefore be said that 0.3 % Nd concentration is the maximum dopant concentration of ZrO_2 for Nd to act as efficient electron trap and limit electron recombination **[17]**. Bare ZrO_2 exhibited the least photocatalytic activity.

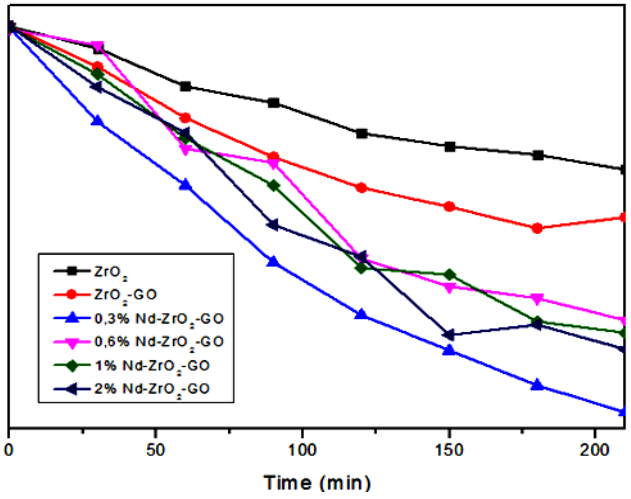

Fig. 7. Degradation profile of Nd doped ZrO_2-GO.

In general, photodegradation reaction of organic compounds can be described by the Langmuir–Hinshelwood model, where the photocatalytic activity of the catalyst can be evaluated using the equation:

$$\ln Co/C = kt$$

where, Co/C is the normalized Eosin Y concentration, t is the reaction time, and k is the apparent reaction rate constant. The kinetics of Eosin Y degradation was obtained by plotting C/Co versus time. All the nanocomposites show better degradation efficiency than zirconium.

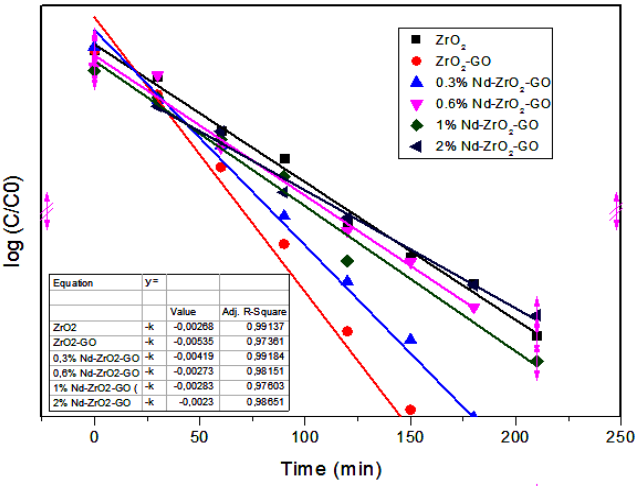

Fig. 8. Kinetics for the degradation of Eosin Y by Nd doped ZrO_2-GO catalysts.

Because of its pseudo-first kinetic order reaction, log (Co/C) versus time **(Fig. 8)** should be linear. These linear relationships are confirmed by **Fig. 8** and good correlation ratio was (R^2>0.97) obtained. The K value of 0.3% Nd-ZrO_2-GO is 4.19×10^{-3} min^{-1}. This value is much higher than that of ZrO_2 (2.88×10^{-3}). Thus 0.3% Nd-ZrO_2-GO degraded

the dye at a faster rate compared to other catalysts with the ZrO_2 operating at the lowest rate.

Nd doped-ZrO_2-GO nanocomposites have been observed to be better catalysts compared too bare ZrO_2, with 0.3% Nd-ZrO_2-GO being the best performing catalyst. These performances are explained by synergic effects of GO and Nd in the composites.

Conclusion

The homogenous co-precipitation method was successfully used to synthesize nanosized ZrO_2 and Nd doped ZrO_2-GO with varying weight percent concentration of Nd. This was confirmed by the various characterization techniques. XRD analysis revealed the amorphous nature of the nanocomposites. The UV-visible absorption spectra of the samples revealed that modification of ZrO_2 using Nd and GO resulted in enhanced visible light absorption of ZrO_2. The Nd doped ZrO_2-GOwere better catalysts against the degradation of Eosin Y dye compared to the bare ZrO_2. From all of the nanocomposites, 0.3 % Nd-ZrO_2-GOwas found to be the best composite for effective degradation of the dye under irradiated solar light. The enhance photocatalytic performance of Nd doped ZrO_2-GO nanocomposites can be attributed to the efficient photosensitized electron booster along with repressed electron recombination due to electron transfer process with GO as electron transporter and collector. The followed method may extend to fabricate graphene based nanocomposite and put his candidature in the field of materials science for sensor, catalysis and fabrication of electronic device fabrication.

Acknowledgement

The authors wish to thank the Faculty of Science, University of Johannesburg, South Africa, National Research Foundation and Water Research Commission of South Africa for providing financial support to carry out this work. SKS and ESA also acknowledge financial support from the Global Excellence and Stature fellowship from the University of Johannesburg.

Authors Contribution

The authors MM and WWA Anku have equal contribution to prepare this manuscript.

Reference

1. Hoffmann, M.R; Martin, S.T.; Choi, W.; Bahnemann, D.W.; *Chemical reviews*, **1995**, *95*, 69. **DOI:** 1 0.1021/cr00033a004
2. Anku, W.W.; Oppong, S.O.; Shukla, S.K.; Govender, P.P.; Acta Chim. Slov., **2016**, *63*, 380.
3. Fujishima, A.; Zhang, X.; Tryk, D.A.; *Surface Science Reports* **2008**, *63*, 515. **DOI:** 10.1016/j.surfrep.2008.10.001
4. Li, W.X.; *Journal of the Australian Ceramic Society*, 2013, *49*, 41.
5. Garcia, J.C.; Scolfaro, L.M.R.; Lino, A.T.; Freire, V.N.; Farias, G.A.; Silva, C.C.; da Silva Jr, E.F.; *Journal of applied physics*, **2006**, *100*, 104103.
6. Emeline, A.; Kataeva, G.V.; Litke, A.S.; Rudakova, A.V.; Ryabchuk, V.K.; Serpone, N.; *Langmuir*, **1998**, *14*, 5011. **DOI:** 10.1021/la980083l
7. Parlak, O.; Beyazit, S.; Tse-Sum-Bui, B.; Haupt, K.; Turner, A.P.F.; Tiwari, A.; *Nanoscale*, **2016**, *8*, 9976. **DOI:** 10.1039/c6nr02355j
8. Parlak, O.; Turner, A.P.F.; Tiwari, A.; *J. Mater. Chem. B.*, **2015**, *3*, 7434. **DOI:** 10.1039/C5TB01355K
9. Tiwari, SK.; Kumar, V.; Huczko, A.; Oraon, R.; Adhikari, AD.; Nayak, GC.; *Critical Reviews in Solid State and Materials Science* **2016**. Article in Press. **DOI:** 10.1080/10408436.2015.1127206
10. Jayakumar, S.; Ananthapadmanabhan, P.V.; Perumal, K.; Thiyagarajan, T.K.; Mishra, S.C.; Su, L.T.; Guo, J.; *Materials Science and Engineering: B*, **2011**, *176*, 894.
11. Shevchenko, V.Y.; Glushkova, V.B.; Panova, T.I.; Podzorova, L.I.; Il'icheva, A.A. Lapshin, A.E.; *Inorganic materials*, **2001**, *37*, 692. **DOI:** 10.1023/A: 1017626107197
12. Landau, L.D.; *Physikalische Zeitschrift der Sowjetunion*, **1933**, *3*, 664.
13. Hummers, W.; Offeman, R.; *Journal of the American Chemical Society*, **1958**, *80*, 1339.
14. Agorku, E.S.; Mamo, M.A.; Mamba, B.B.; Pandey, A.C.; Mishra, A.K.; *Journal of Porous Materials*, **2015**, 22, 47.
15. Bhargava, R.N.; Gallagher, D.; Hong, X.; Nurmikko, A.; *Physical Review Letters*, **1994**, *72*, 416. **DOI:** 10.1016/j.mseb.2011.05.013
16. Wang, Z.; Huang, B.; Dai, Y.; Liu, Y.; Zhang, X.; Qin, X.; Cheng, H.; *CrystEngComm*, **2012**, *14*, 1687. **DOI:** 10.1039/C1CE06193C
17. Zhang, Y.; Zhang, N.; Tang, Z.R.; Xu, Y.J.; *ACS Nano*, **2012**, *6*, 9777.

Graphical abstract